AIP | Applied Physics Letters

Ultra-low thermal conductivity of ellipsoidal TiO2 nanoparticle films

Patrick E. Hopkins, Manish Mittal, Leslie M. Phinney, Anne M. Grillet, and Eric M. Furst

Citation: Appl. Phys. Lett. **99**, 133106 (2011); doi: 10.1063/1.3644987
View online: http://dx.doi.org/10.1063/1.3644987
View Table of Contents: http://apl.aip.org/resource/1/APPLAB/v99/i13
Published by the American Institute of Physics.

Related Articles

Large reduction in thermal conductivity for Ge quantum dots embedded in SiO2 system
Appl. Phys. Lett. 101, 251913 (2012)

A “2-omega” technique for measuring anisotropy of thermal conductivity
Rev. Sci. Instrum. 83, 124903 (2012)

Thermal conductivity of nano-grained SrTiO3 thin films
Appl. Phys. Lett. 101, 231908 (2012)

The c-axis thermal conductivity of graphite film of nanometer thickness measured by time resolved X-ray diffraction
Appl. Phys. Lett. 101, 233108 (2012)

Thermal rectification reversal in carbon nanotubes
J. Appl. Phys. 112, 103515 (2012)

Additional information on Appl. Phys. Lett.

Journal Homepage: http://apl.aip.org/
Journal Information: http://apl.aip.org/about/about_the_journal
Top downloads: http://apl.aip.org/features/most_downloaded
Information for Authors: http://apl.aip.org/authors

ADVERTISEMENT

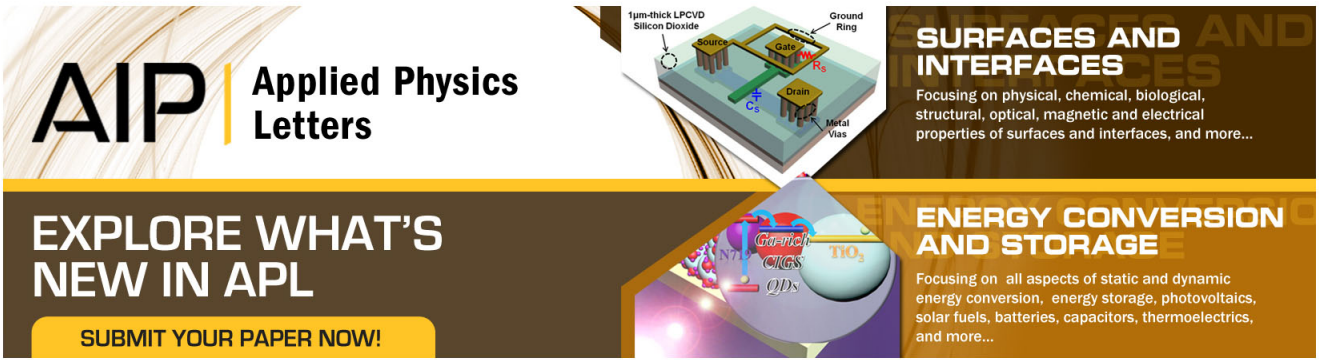

Ultra-low thermal conductivity of ellipsoidal TiO_2 nanoparticle films

Patrick E. Hopkins,[1,2,a)] Manish Mittal,[3] Leslie M. Phinney,[2] Anne M. Grillet,[2] and Eric M. Furst[3]
[1]*Department of Mechanical and Aerospace Engineering, University of Virginia, Charlottesville, Virginia 22904, USA*
[2]*Engineering Sciences Center, Sandia National Laboratories, Albuquerque, New Mexico 87185, USA*
[3]*Department of Chemical Engineering and Center for Molecular and Engineering Thermodynamics, University of Delaware, Newark, Delaware 19716, USA*

(Received 13 July 2011; accepted 9 September 2011; published online 27 September 2011)

We report on the thermal conductivity of a series of convectively assembled, anisotropic titania (TiO_2) nanoparticle films. The TiO_2 films are fabricated by flow coating a suspension of ellipsoidal colloidal nanoparticles, resulting in structured films with tailored orientational order. The thermal conductivities depend on nanoparticle orientation and can be less than amorphous TiO_2 films due to inter-nanoparticle boundary scattering. This nanoparticle ordering presents a unique method for manipulating the thermal conductivity of nanocomposites. © *2011 American Institute of Physics*. [doi:10.1063/1.3644987]

Low thermal conductivity nanomaterials have been created by tailoring the structure and interface densities nanosystems.[1–3] However, decreasing the thermal conductivity is often achieved through undesirable processing or material changes. For example, fabrication and construction of nanoparticle composite films can be intricate and costly, thereby creating difficulties in scaling up the production of materials with unique thermal properties for actual applications. Typical approaches to reducing the thermal conductivity in nanosystems rely on increasing the density of nanoparticle inclusions or interfaces.[4] A recent theoretical study[5] predicted that spherical, cubically-packed nanoparticles will have thermal conductivities below the minimum limit[6] due to a large resistance from interfacial scattering between the nanoparticles. Presumably, with asymmetrically shaped nanoparticle arrangements, the frequency of the interfacial scattering events can be tuned, thereby introducing avenues for manipulation, and reduction, of thermal transport.

In this work, we demonstrate an approach to fabricate films of closely packed titania nanoparticles that exhibit thermal conductivity below the theoretical minimum limit, depending on nanoparticle orientation. The thermal conductivities, which are measured with time domain thermoreflectance (TDTR), are dependent on nanoparticle orientational order, which is controllable from the flow coating processes. The measured thermal conductivities of the nanoparticle films have similar magnitudes of thermal conductivity as an amorphous film but temperature trends similar to a polycrystalline sputtered film, indicating that the phonon transport in the nanoparticle films is not limited by the interatomic spacing or lack of periodicity as in the amorphous film.

Ellipsoidal titania particles are synthesized by a gel-sol chemistry in the presence of ethylenediamine.[7] The polycrystalline nanoparticles have an equatorial radius $a = 24 \pm 4$ nm, a polar radius $b = 130 \pm 31$ nm, and a density of 2.74 ± 0.10 g cm^{-3}. Films of titania particles are deposited on aluminum coated glass slides by flow coating a suspension of ellipsoidal colloidal titantia nanoparticles.[8,9] Briefly, a stable colloidal suspension of the titania nanoparticles suspended in ultra-pure water (resistivity ≥ 18.2 MΩ cm) is confined between the substrate and a glass blade positioned 200 μm above and at 25° inclination. The nanoparticle volume fractions in the suspensions are below ($\phi = 0.24$, film 1) and above ($\phi = 0.52$, films 2 and 3) the isotropic-nematic transition, $\phi^* \approx 0.4$ (note that ϕ is the nanoparticle volume fraction of suspension used to flow coat the film, not the nanoparticle packing density of the film after assembly). The substrate is translated by a computer controlled motorized stage at a velocity, v, of 125 μm s^{-1} (films 1 and 2) or 750 μs^{-1} (film 3). Prior to coating, the substrate is washed thoroughly with ultra-pure water, followed by plasma cleaning (Model PDC-32G, Harrick Plasma). The film structure depends on both the nanoparticle volume fraction in the suspensions (ϕ) and the substrate velocity (v) during the coating. The packing fraction of the final film does not vary substantially, as demonstrated in our earlier study of the film deposition.[8] A detailed description of the effect of experimental parameters on the film structure is described elsewhere.[8] The thicknesses of films 1, 2, and 3 are 150, 370, and 650 nm, respectively. Scanning electron microscopy (SEM) images in Fig. 1 show example film structures for samples used in this study. The nanoparticles in the films exhibit different degrees of orientational order. The order parameter, P_2, is determined from the SEM image analysis using $P_2 = \sum_{i=1}^{N} \cos(2\theta_i)/N$, where θ_i is the angle of particle i relative to the flow coating direction and N is the number of particles in each image. The order parameters of films 1, 2, and 3 are $P_2 = 0.335$, 0.73, and 0.91, respectively. Indeed, the order parameter represents the ordering in-plane where the thermal transport measurements are taken in the out-of-plane (or cross plane direction). However, the ordering that we report in-plane, although not a direct measure of the out-of-plane order, is related to, and a qualitative indication of, the ordering and packing out-of-plane.

We measured the thermal conductivity, κ, of the thin films of convectively assembled TiO_2 nanoparticles with TDTR from 77–300 K.[10–12] In our TDTR experiments, we focus our pump and probe beams through the glass slide onto the surface of the Al film at the glass/Al interface.[13–15] We use a bidirectional

a)Electronic mail: phopkins@virginia.edu.

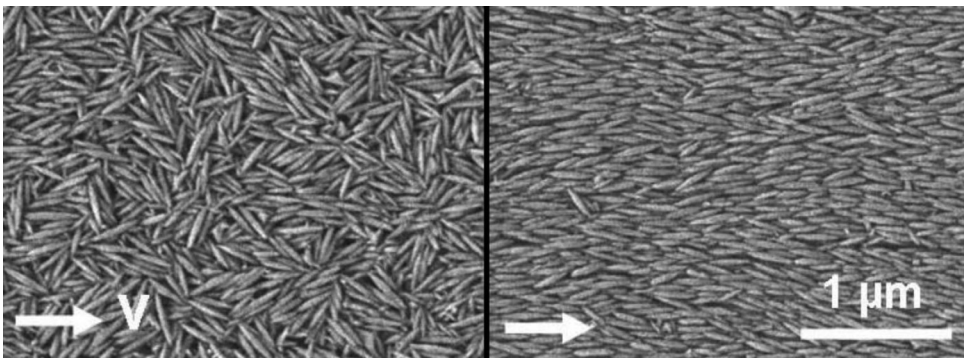

FIG. 1. SEM images of the deposited films. (Left) Film 1—a disordered film: $\phi = 0.24$, $v = 125\,\mu\text{m s}^{-1}$. (Right) Film 3—an ordered film: $\phi = 0.52$, $v = 1500\,\mu\text{m s}^{-1}$. The scale bar is $1.0\,\mu\text{m}$.

heat transfer model to extract the thermal conductivity of the TiO_2 nanoparticle films from the thermal conduction through the glass.[15] We account for the finite thickness of the nanoparticle films in our thermal model and assume an insulated boundary condition at the exposed surface of the film. Our TDTR tests are all conducted in a vacuum less than 1.0 mTorr, ensuring negligible thermal transport by the air in the space not occupied by the nanoparticles.[16] The average thermal conductivities of three films as a function of temperature are shown in Fig. 2. For comparison, we also plot the thermal conductivity of bulk, single crystalline TiO_2 (Ref. 17), a polycrystalline sputtered film with 17 nm grain size,[18] and an amorphous TiO_2 film.[19] We estimate the grain sizes in the TiO_2 nanoparticles from high resolution TEM images as ~15 nm. The thermal conductivities of the nanoparticle based films in this study are significantly lower, nearly an order of magnitude in some cases, than the sputtered TiO_2 film with similar grain sizes. The measured thermal conductivities of the nanoparticle films have similar magnitudes of κ as the amorphous film but temperature trends similar to the polycrystalline sputtered film, indicating that the phonon transport in the nanoparticle films is not limited by the interatomic spacing or lack of periodicity as in the amorphous film. This implies that three-phonon scattering and boundary scattering are still dominant phonon scattering events in these nanoparticle films with low thermal conductivity.

To investigate the phonon mechanisms contributing to the thermal conductivities of these TiO_2 close-packed nanoparticle films, we model the thermal conductivity in TiO_2 with an approach similar to that outlined by Mingo.[20] In short, we treat the TiO_2 samples as isotropic Debye media and model the thermal conductivity with

$$\kappa_p = \frac{1}{3}\sum_j \int_{\omega_j} C_j(\omega) v_j^2 \tau_j(\omega) d\omega, \qquad (1)$$

where C_j is the volumetric heat capacity per normal mode at frequency ω, v_j is the phonon velocity, and τ_j is the scattering time, and the summation is over the j polarizations. We make the Debye approximation for TiO_2 and take the longitudinal and transverse phonon velocities as 9200 and 5100 ms^{-1}, respectively.[18] Note that this approach of modeling the thermal conductivity of bulk TiO_2 under the Debye approximation was also successfully employed by Lee *et al.*[18] We fit Eq. (1) to the thermal conductivity of bulk TiO_2 to determine the intrinsic three-phonon and impurity scattering times. The best fit is shown as the black line through the bulk TiO_2 data in Fig. 2.

To understand the phonon scattering mechanisms contributing to the observed thermal conductivities in the nanoparticle films, we model the thermal conductivity in an individual nanoparticle with Eq. (1) using the three-phonon and impurity scattering times determined from the bulk fit and incorporate an additional grain boundary scattering time given by $\tau_{g,j} = d/v_j$, where we approximate d in the nanoparticles as 15 nm from high resolution TEM of the nanoparticles, as previously mentioned. This approach, however, does not explain the different observed κ in the representative ordered (film 3) and disordered (film 1) films. To explain this, we consider the effect of thermal boundary resistance, R, between the nanoparticles by taking the overall thermal conductivity of the nanoparticle film as $\kappa = \kappa_p/(1 + R\kappa_p/L)$, where L is the characteristic distance that the

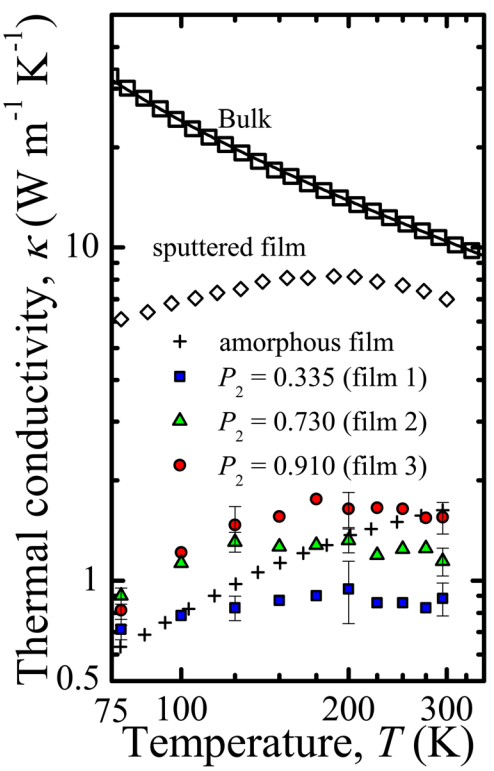

FIG. 2. (Color online) Thermal conductivities of three different films: an ordered film (film 3), a disordered film (film 1), and a moderately ordered/disordered film (film 2) along with the thermal conductivity of bulk, single crystalline TiO_2 (Ref. 17), a polycrystalline sputtered film with 17 nm grain size (Ref. 18), and an amorphous TiO_2 film (Ref. 19). Representative error bars are shown, which represent the standard deviation calculated from the 5 different measurements on each sample.

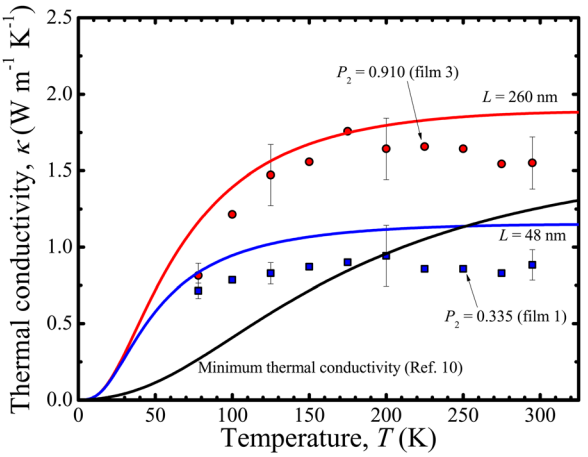

FIG. 3. (Color online) Thermal conductivity of film 3 (ordered) and film 1 (disordered) as a function of temperature. The temperature trends of the experimental data are different than those predicted by the minimum limit. We model the thermal conductivity of the films by considering Umklapp, impurity and grain boundary scattering, and interparticle thermal boundary resistance. $L = 260$ nm and $L = 48$ nm correspond to the length and width of a TiO_2 nanoparticle, respectively, and are the bounds on the distance, a phonon can propagate before scattering.

phonons traverse in the nanoparticle before scattering at the nanoparticle-nanoparticle interface and κ_p is calculated from Eq. (1).[21] We estimate the thermal boundary resistance as $R = 2.0 \times 10^{-8}$ m^2 KW^{-1}, an average value for resistances involving oxides,[12,21] and consider two limiting cases of phonons propagating the length (260 nm) or width (48 nm) of the nanoparticle before experiencing an interfacial scattering event. As seen in Fig. 3, the models for the ordered film with the highest thermal conductivity (film 3) and the disordered films with the lowest thermal conductivity (film 1) describe the measured data and trends with temperature acceptably. For comparison, we also show the theoretical minimum thermal conductivity of TiO_2 using the measured density of the films (2.74 g cm^{-3}).[6] The theoretical minimum thermal conductivity does not capture the temperature trends in the nanoparticle packed films. The temperature trends of the nanoparticle films, which are indicative of a polycrystalline material and similar to the polycrystalline sputtered film shown in Fig. 2, are, however, well predicted by the model in Eq. (1) when accounting for Umklapp scattering, which means that three-phonon scattering events are still playing a role in the thermal transport. The magnitude of the thermal conductivity is lowered by particle-particle interface scattering, with this scattering rate increasing with nanoparticle disorder. This model elucidates the essential mechanisms underlying the thermal transport in these nanoparticle films: i.e., three-phonon and boundary scattering. The frequency of the boundary scattering, which is dictated by the nanoparticle alignment and order and in turn is controllable during coating, results in thermal conductivities less than the theoretical minimum limit for a titania film with the same density. Although not pursued here, a more detailed model could study how the nanoparticle contact areas affect the boundary and constriction resistances, and roles of these resistances in thermal conductivity.[5]

We reiterate that the order parameter that we report is based on the order in the in plane direction where the thermal transport that we measure via TDTR is cross-plane. For the most part, we expect the ordering in the in-plane direction to be a qualitative indication of the relative ordering in the cross-plane direction when comparing amongst the various samples, as we have observed in our image analysis. However, a more thorough, quantitative structural analysis of the in-plane vs. cross-plane ordering must be pursued in future studies to truly correlate the thermal transport to nanoparticle orientation, and therefore fully exploit the potential for thermal tunability of nanoparticle films.

In summary, we report on the thermal conductivity of a series of convectively assembled, anisotropic titania (TiO_2) nanoparticle films. The thermal conductivities of these nanoparticle films are nearly an order of magnitude less than that of polycrystalline TiO_2 films with similar grain sizes. The thermal conductivities are dependent on nanoparticle orientational order, and films with more randomly oriented particles exhibit thermal conductivities less than amorphous films. The temperature trends in the thermal conductivities suggest that, in addition to Umklapp and grain boundary scattering in the TiO_2 nanoparticles, the thermal boundary resistance between individual nanoparticles is contributing to the thermal conductivity of these convectively assembled TiO_2 nanoparticle thin films.

Sandia is a multiprogram laboratory operated by Sandia Corporation, a wholly owned subsidiary of Lockheed Martin Corporation, for the United States Department of Energy National Nuclear Security Administration under Contract No. DE-AC04-94AL85000. E.M.F. acknowledges the financial support of the U.S. Department of Energy, Basic Energy Sciences (Grant No. DE-FG02-09ER46626).

[1]R. M. Costescu, D. G. Cahill, F. H. Fabreguette, Z. A. Sechrist, and S. M. George, Science **303**, 989 (2004).
[2]C. Chiritescu, D. G. Cahill, N. Nguyen, D. Johnson, A. Bodapati, P. Keblinski, and P. Zschack, Science **315**, 351 (2007).
[3]G. Pernot, M. Stoffel, I. Savic, F. Pezzoli, P. Chen, G. Savelli, A. Jacquot, J. Schumann, U. Denker, I. Monch, C. Deneke, O. G. Schmidt, J. M. Rampnoux, S. Wang, M. Plissonnier, A. Rastelli, S. Dilhaire, and N. Mingo, Nature Mater. **9**, 491 (2010).
[4]D. G. Cahill, W. K. Ford, K. E. Goodson, G. D. Mahan, A. Majumdar, H. J. Maris, R. Merlin, and S. R. Phillpot, J. Appl. Phys. **93**, 793 (2003).
[5]R. S. Prasher, Phys. Rev. B **74**, 165413 (2006).
[6]D. G. Cahill, S. K. Watson, and R. O. Pohl, Phys. Rev. B **46**, 6131 (1992).
[7]T. Sugimoto, X. W. Zhou, and A. Muramatsu, J. Colloid Interface Sci. **259**, 53 (2003).
[8]M. Mittal, R. K. Niles, and E. M. Furst, Nanoscale **2**, 2237 (2010).
[9]M. Mittal and E. M. Furst, Adv. Funct. Mater. **19**, 3271 (2009).
[10]D. G. Cahill, K. E. Goodson, and A. Majumdar, J. Heat Transfer **124**, 223 (2002).
[11]D. G. Cahill, Rev. Sci. Instrum. **75**, 5119 (2004).
[12]P. E. Hopkins, J. R. Serrano, L. M. Phinney, S. P. Kearney, T. W. Grasser, and C. T. Harris, J. Heat Transfer **132**, 081302 (2010).
[13]Z. Ge, D. G. Cahill, and P. V. Braun, Phys. Rev. Lett. **96**, 186101 (2006).
[14]A. Schmidt, M. Chiesa, X. Chen, and G. Chen, Rev. Sci. Instrum. **79**, 064902 (2008).
[15]P. E. Hopkins, B. Kaehr, L. M. Phinney, T. P. Koehler, A. M. Grillet, D. Dunphy, F. Garcia, and C. J. Brinker, J. Heat Transfer **133**, 061601 (2011).
[16]S. Spagnol, B. Lartigue, and A. Trombe, J. Heat Transfer **131**, 074501 (2009).
[17]*Thermal Conductivitiy—Nonmetallic Solids*, Thermophysical Properties of Matter, Vol. 2 (IFI/Plenum, New York, 1970).
[18]S. M. Lee, D. G. Cahill, and T. H. Allen, Phys. Rev. B **52**, 253 (1995).
[19]D. G. Cahill and T. H. Allen, Appl. Phys. Lett. **65**, 309 (1994).
[20]N. Mingo, Phys. Rev. B **68**, 113308 (2003).
[21]S. M. Lee and D. G. Cahill, J. Appl. Phys. **81**, 2590 (1997).